#### **MAGNETISM**

# Giant tunneling magnetoresistance in spin-filter van der Waals heterostructures

Tiancheng Song<sup>1\*</sup>, Xinghan Cai<sup>1\*</sup>, Matisse Wei-Yuan Tu<sup>2</sup>, Xiaoou Zhang<sup>3</sup>, Bevin Huang<sup>1</sup>, Nathan P. Wilson<sup>1</sup>, Kyle L. Seyler<sup>1</sup>, Lin Zhu<sup>4</sup>, Takashi Taniguchi<sup>5</sup>, Kenji Watanabe<sup>5</sup>, Michael A. McGuire<sup>6</sup>, David H. Cobden<sup>1</sup>, Di Xiao<sup>3</sup> $\dagger$ , Wang Yao<sup>2</sup> $\dagger$ , Xiaodong Xu<sup>1,4</sup> $\dagger$ 

Magnetic multilayer devices that exploit magnetoresistance are the backbone of magnetic sensing and data storage technologies. Here, we report multiple-spin-filter magnetic tunnel junctions (sf-MTJs) based on van der Waals (vdW) heterostructures in which atomically thin chromium triiodide (Crl<sub>3</sub>) acts as a spin-filter tunnel barrier sandwiched between graphene contacts. We demonstrate tunneling magnetoresistance that is drastically enhanced with increasing Crl<sub>3</sub> layer thickness, reaching a record 19,000% for magnetic multilayer structures using four-layer sf-MTJs at low temperatures. Using magnetic circular dichroism measurements, we attribute these effects to the intrinsic layer-by-layer antiferromagnetic ordering of the atomically thin Crl<sub>3</sub>. Our work reveals the possibility to push magnetic information storage to the atomically thin limit and highlights Crl<sub>3</sub> as a superlative magnetic tunnel barrier for vdW heterostructure spintronic devices.

any two-dimensional (2D) materials can be incorporated into artificial heterostructures without the need for lattice matching. These materials thus provide a platform for exploring emerging phenomena and device function at the designed atomic interfaces (1, 2). However, magnetic memory and processing applications were out of reach in van der Waals (vdW) heterostructures before the

recent discovery of suitable 2D magnetic materials (3-10). One of these is the magnetic insulator chromium triiodide (CrI<sub>3</sub>), which in bilayer form has been found to possess a layered-antiferromagnetic ground state. Magneto-optical Kerr effect (MOKE) measurements suggest that the spins align ferromagnetically out of plane within each layer but antiferromagnetically between layers, resulting in vanishing net magnetization (Fig. 1A, left) (3).

This lavered-antiferromagnetic ordering makes CrI<sub>3</sub> desirable for realizing atomically thin magnetic multilayer devices. When the magnetizations of the two layers in a bilayer are switched between antiparallel (Fig. 1A, left) and parallel states (Fig. 1A, middle and right), giant tunneling magnetoresistance (TMR) is produced by the double spin-filtering effect (11, 12). In general, spin filters, which create and control spin-polarized currents, are the fundamental element in magnetic multilayer devices, such as spin valves (13-15), magnetic tunnel junctions (MTJs) (16-21), and double spin-filter MTJs (sf-MTJs) (11, 12). Compared with the existing magnetic multilayer devices that require different choices of (metallic or insulating) magnets and spacers, the layeredantiferromagnetic structure in bilayer CrI3 avoids the need for fabricating separate spin filters with spacers. This guarantees sharp atomic interfaces between spin filters, crucial for achieving large

An even more intriguing possibility arises if the intrinsic layered-antiferromagnetic structure of CrI<sub>3</sub> extends beyond the bilayer. In this case,

<sup>1</sup>Department of Physics, University of Washington, Seattle, WA 98195, USA. <sup>2</sup>Department of Physics and Center of Theoretical and Computational Physics, University of Hong Kong, Hong Kong, China. <sup>3</sup>Department of Physics, Carnegie Mellon University, Pittsburgh, PA 15213, USA. <sup>4</sup>Department of Materials Science and Engineering, University of Washington, Seattle, WA 98195, USA. <sup>5</sup>National Institute for Materials Science, Tsukuba, Ibaraki 305-0044, Japan. <sup>6</sup>Materials Science and Technology Division, Oak Ridge National Laboratory, Oak Ridge, TN 27231 USA.

\*These authors contributed equally to this work.

†Corresponding author. Email: xuxd@uw.edu (X.X.); wangyao@ hku.hk (W.Y.); dixiao@cmu.edu (D.X.)

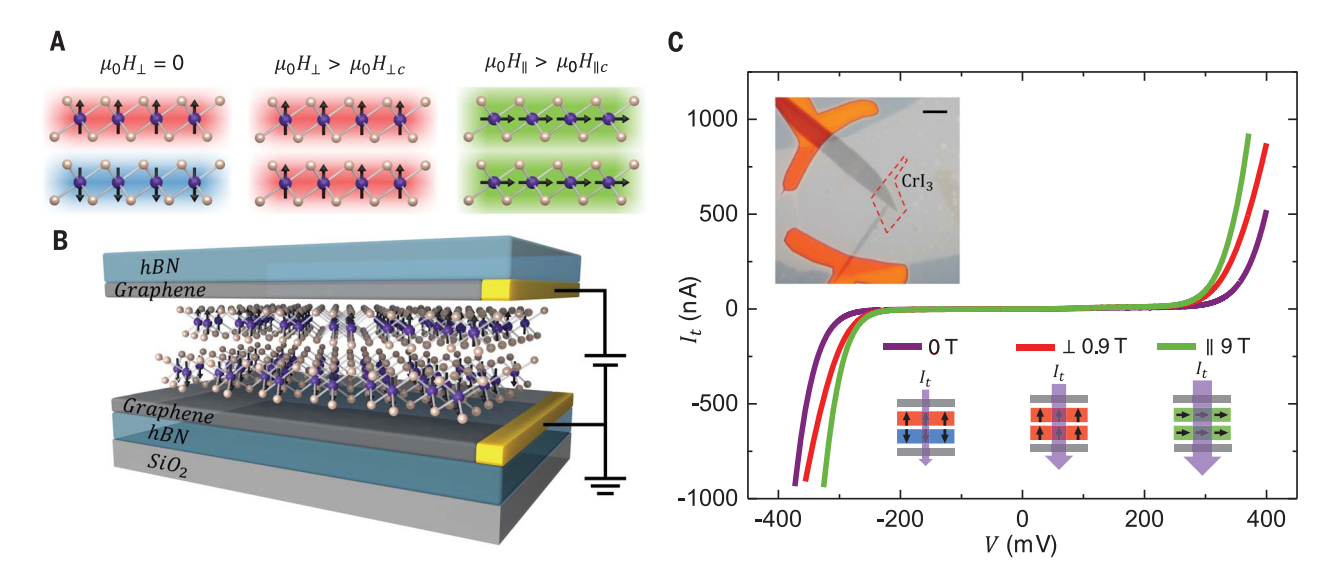


**Fig. 1. Spin-filter effects in layered-antiferromagnetic Crl**<sub>3</sub>. **(A)** Schematic of magnetic states in bilayer Crl<sub>3</sub>. (Left) Layered-antiferromagnetic state, which suppresses the tunneling current at zero magnetic field. (Middle and right) Fully spin-polarized states with out-of-plane and in-plane magnetizations, which do not suppress it. **(B)** Schematic of 2D spin-filter magnetic tunnel

junction (sf-MTJ), with bilayer  $Crl_3$  functioning as the spin-filter sandwiched between few-layer graphene contacts. (**C**) Tunneling current of a bilayer  $Crl_3$  sf-MTJ at selected magnetic fields. (Top inset) Optical microscope image of the device (scale bar, 5  $\mu$ m). The red dashed line shows the position of the bilayer  $Crl_3$ . (Bottom) Schematic of the magnetic configuration for each  $I_f$ -V curve.

every layer should act as another spin filter oppositely aligned in series, greatly enhancing the sf-TMR as the number of layers increases. The associated multiple magnetic states may also enable multiple magnetoresistance states for potentially encoding information in an individual sf-MTJ device. Moreover, being insulators, atomically thin CrI<sub>3</sub> single crystals can be integrated into vdW heterostructures as tunnel barriers in place of nonmagnetic dielectrics, such as hexagonal boron nitride (hBN) (22, 23) or transition metal dichalcogenides (24), adding magnetic switching functionality. The realization of such vdW heterostructure sf-MTJs could produce novel 2D magnetic interface phenomena (25) and enable spintronics components such as spin current sources and magnetoresistive random-access memory (MRAM) (26).

Here, we demonstrate vdW-engineered sf-MTJs based on atomically thin  ${\rm CrI_3}$  with extraordinarily large sf-TMR. Figure 1B shows the essential structure of the sf-MTJ, which consists of two few-layer graphene contacts separated by a thin  ${\rm CrI_3}$  tunnel barrier. The sf-MTJ is sandwiched between two hexagonal boron nitride (hBN) flakes to avoid degradation. We have made and in-

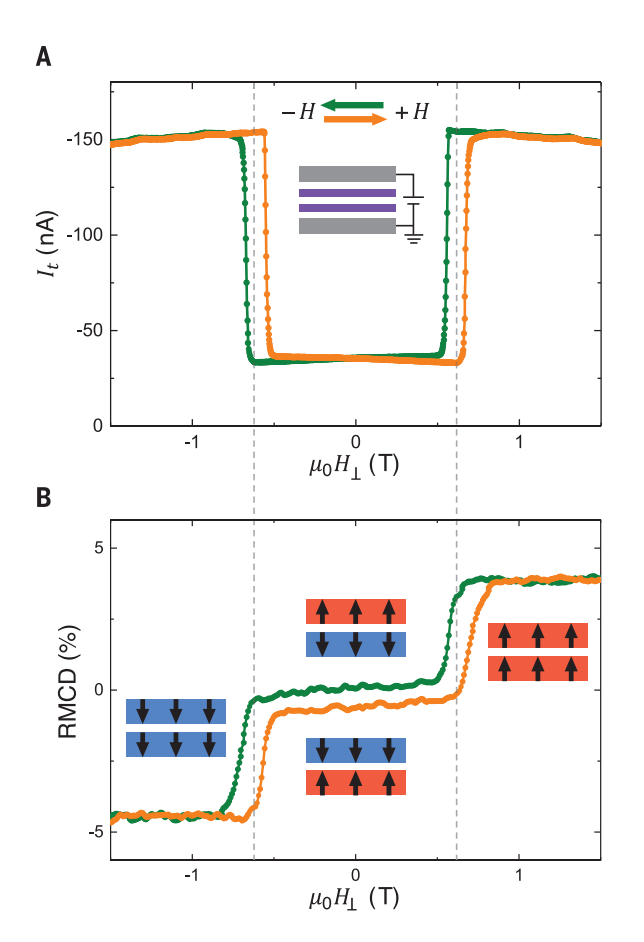
vestigated devices with bilayer, trilayer, and fourlayer CrI<sub>3</sub>. All measurements were carried out at a temperature of 2 K. unless otherwise specified.

We begin with the case of bilayer CrI<sub>3</sub>. The inset of Fig. 1C is an optical micrograph of a device with the structure illustrated in Fig. 1B, obtained by stacking exfoliated 2D materials using a dry-transfer process in a glovebox (27). The tunneling junction area is less than  $\sim 1 \mu m^2$ to avoid effects caused by lateral magnetic domain structures (3, 4). Figure 1C shows the tunneling current  $(I_t)$  as a function of DC bias voltage (V) at selected magnetic fields ( $\mu_0H$ ) (27). Unlike in tunneling devices using nonmagnetic hBN as the barrier (22, 23), it has a strong magnetic field dependence. As shown in Fig. 1C,  $I_t$  is much smaller at  $\mu_0 H = 0$  T (purple trace) than it is in the presence of an out-of-plane field ( $\mu_0 H_{\parallel}$ , red trace) or an in-plane field ( $\mu_0 H_{\parallel}$ , green trace). This magnetic field-dependent tunneling current implies a spin-dependent tunneling probability related to the field-dependent magnetic structure of bilayer CrI<sub>3</sub>.

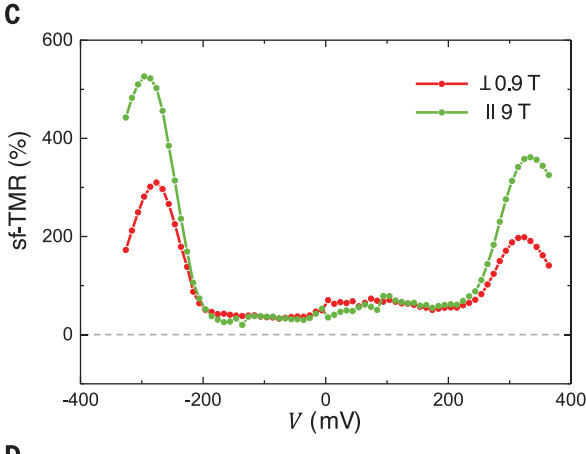
To investigate the connection between the bilayer  $CrI_3$  magnetic states and the magnetoresistance, we measured  $I_t$  as a function of  $\mu_0H_\perp$ 

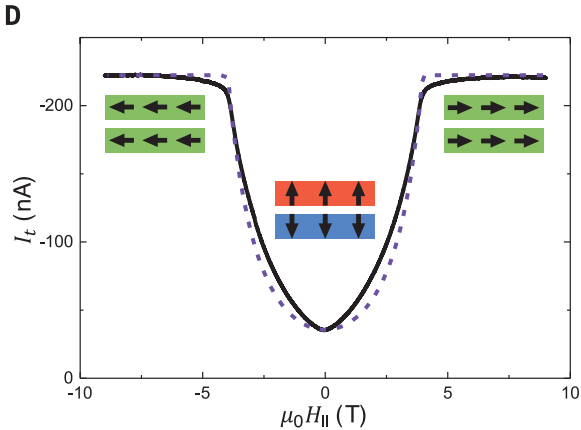
at a particular bias voltage (-290 mV). The green and orange curves in Fig. 2A correspond to decreasing and increasing magnetic fields, respectively.  $I_t$  exhibits plateaus with two values, about -36 nA and -155 nA. The lower plateau is seen at low fields, and there is a sharp jump to the higher plateau when the magnetic field exceeds a critical value. We also employed reflective magnetic circular dichroism (RMCD) to probe the out-of-plane magnetization of the bilayer CrI3 near the tunneling area. Figure 2B shows the RMCD signal as a function of  $\mu_0 H_{\perp}$  under similar experimental conditions to the magnetoresistance measurements (27). The signal is small at low fields, corresponding to a layeredantiferromagnetic ground state ( $\uparrow\downarrow$  or  $\downarrow\uparrow$ ), where the arrows indicate the out-of-plane magnetizations in the top and bottom layers, respectively. As the magnitude of the field increases, there is a step up to a larger signal corresponding to the fully spin-polarized states ( $\uparrow \uparrow$  and  $\downarrow \downarrow$ ), consistent with earlier MOKE measurements on bilayer CrI<sub>3</sub> (3). Additional bilayer device measurements can be found in (27).

A direct comparison of  $I_t$  and RMCD measurements provides the following explanation of the



**Fig. 2. Double spin-filter MTJ from bilayer CrI<sub>3</sub>.** (**A**) Tunneling current as a function of out-of-plane magnetic field  $(\mu_0 H_\perp)$  at a selected bias voltage (–290 mV). Green (orange) curve corresponds to decreasing (increasing) magnetic field. The junction area is about 0.75  $\mu$ m<sup>2</sup>. (**B**) Reflective magnetic circular dichroism (RMCD) of the same device





at zero bias. Insets show the corresponding magnetic states. **(C)** Extracted sf-TMR ratio as a function of bias based on the  $I_t$ -V curves in Fig. 1C. **(D)** Tunneling current as a function of in-plane magnetic field ( $\mu_0H_{\parallel}$ ) (black) at a selected bias voltage (–290 mV) with simulations (dashed purple). Insets show the corresponding magnetic states.

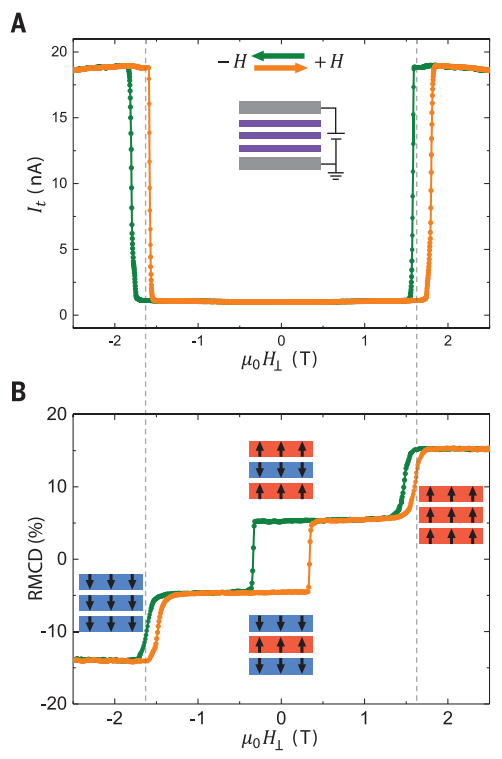
giant sf-TMR: In the  $\uparrow \downarrow$  or  $\downarrow \uparrow$  states at low field, the current is small because spin-conserving tunneling of an electron through the two layers in sequence is suppressed. The step in  $I_t$  occurs when the magnetic field drives the bilayer into the  $\uparrow\uparrow$  and  $\downarrow\downarrow$  states and this suppression is removed. This is known as the double spinfiltering effect (11, 12), and it can be modeled by treating the two monolayers as tunnel-coupled spin-dependent quantum wells (27).

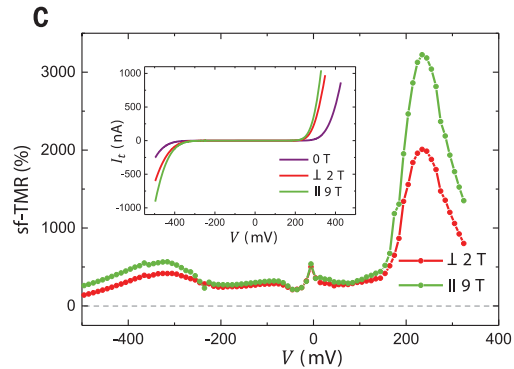
We quantify the sf-TMR by  $(R_{\rm ap} - R_{\rm p})/R_{\rm p}$ , where  $R_{\rm ap}$  and  $R_{\rm p}$  are the DC resistances with antiparallel and parallel spin alignment in bilayer CrI3, respectively, measured at a given bias. Figure 2C shows the value of this quantity as a function of bias extracted from the  $I_tV$ curves in Fig. 1C. The highest sf-TMR achieved is 310% for magnetization fully aligned perpendicular to the plane and 530% for parallel alignment. The sf-TMR decreases as temperature increases and vanishes above the critical temperature at about 45 K (27).

The fact that the sf-TMR for in-plane magnetization is larger than for out-of-plane implies anisotropic magnetoresistance, which is a common feature in ferromagnets (28) and is a sign of anisotropic spin-orbit coupling stemming from the layered structure of CrI<sub>3</sub>. The sf-TMR is also peaked at a certain bias and asymmetric between positive and negative bias. These observations are similar to the reported double sf-MTJs based on EuS thin films, where the asymmetry is caused by the different thickness and coercive fields of the two EuS spin filters (12). Likewise, our data imply that the device lacks up-down symmetry, possibly because the few-layer graphene contacts are not identical in thickness. This broken symmetry also manifests as tilting of the current plateaus (Fig. 2A) and the finite nonzero RMCD value (Fig. 2B) in the layered-antiferromagnetic states (27).

To further investigate magnetic anisotropy and the assignment of magnetic states in the bilayer, we measured  $I_t$  as a function of in-plane magnetic field. As shown in Fig. 2D (black curve),  $I_t$  is smallest at zero field, in the layeredantiferromagnetic state, and smoothly increases with the magnitude of the field. This behavior has a natural interpretation in terms of a spincanting effect. Once the magnitude of  $\mu_0 H_{\parallel}$ exceeds about 4 T, the spins are completely aligned with the in-plane field and  $I_t$  saturates. Simulations of the canting effect to match the data (dashed purple curve) yield a magnetic anisotropy field of 3.8 T (27), much larger than the out-of-plane critical magnetic field of ±0.6 T seen in Fig. 2A. These results therefore both demonstrate and quantify a large out-of-plane magnetic anisotropy in bilayer CrI<sub>3</sub>.

We next consider the trilayer case. Figure 3, A and B, shows  $I_t$  and RMCD, respectively, for a trilayer CrI3 sf-MTJ as a function of out-ofplane field. There are four plateaus in the RMCD signal, at -14%, -5%, 5%, and 15%, the ratio between which is close to -3:-1:1:3. By analogy with the analysis of the ↑↓ and ↓↑ layered-





(A) Tunneling current as a function of out-of-plane magnetic field ( $\mu_0 H_{\perp}$ ) at a selected bias voltage (235 mV). The junction area is about 0.06  $\mu$ m<sup>2</sup>. (**B**) RMCD of the same device at zero bias showing antiferromagnetic

Fig. 3. Giant sf-TMR of a trilayer Crl<sub>3</sub> sf-MTJ.

interlayer coupling. Insets show the corresponding magnetic states. (C) sf-TMR ratio calculated from the  $I_t$  -V data shown in the inset.

antiferromagnetic states in the bilayer, we identify the trilayer ground state as  $\uparrow\downarrow\uparrow$  or  $\downarrow\uparrow\downarrow$  at zero field. We conclude that the interlayer coupling in trilayer CrI<sub>3</sub> is also antiferromagnetic, and the net magnetization in the ground state—and thus the RMCD value-is 1/3 of the saturated magnetization when the applied field fully aligns the three layers (27). The jumps in  $I_t$  and RMCD in Fig. 3, A and B, are caused by the magnetization of an individual layer flipping, similar to what is seen in metallic layered antiferromagnets (29-32).

We deduce that the low current plateau at small fields in Fig. 3A occurs because the two layered-antiferromagnetic states ( $\uparrow\downarrow\uparrow$  and  $\downarrow\uparrow\downarrow$ ) of the trilayer function as three oppositely polarized spin filters in series. Large enough fields drive the trilayer into fully spin-polarized states, which enhances tunneling and gives the high current plateaus. Figure 3C shows the sf-TMR as a function of bias derived from the  $I_t$ -V curves shown in the inset. The peak values are about 2000% and 3200% for magnetization fully aligned perpendicular and parallel to the plane, respectively, revealing a drastically enhanced sf-TMR compared with bilayer devices.

Increasing the CrI<sub>3</sub> thickness beyond three layers unlocks more complicated magnetic configurations. Figure 4, A and B, shows  $I_t$  and RMCD, respectively, for a four-layer device. There are multiple plateaus in each, signifying several magnetic configurations with different effects on the tunneling resistance. The small RMCD signal at low fields, below ~0.8 T, corresponds to the fully antiferromagnetic ground state, either  $\uparrow\downarrow\uparrow\downarrow$  or  $\downarrow\uparrow\downarrow\uparrow$ . The fact that the RMCD is not zero (Fig. 4B) can be attributed to the asymmetry of the layers caused by the fabrication process, as in the bilayer case above (27). As expected, these fully antiferromagnetic states are very effective at suppressing the tunneling current because they act as four oppositely polarized spin filters in series, explaining the very low current plateau at small fields in Fig. 4A. Applying a large enough field fully aligns the  $\downarrow\downarrow\downarrow\downarrow\downarrow$ ), producing the highest plateaus in both  $I_t$  and RMCD. Figure 4C shows the sf-TMR as a function of bias extracted from the  $I_{t}V$ curves in the inset. The peak values are now about 8600% and 19,000% for perpendicular and parallel field, respectively, representing a further enhancement of the sf-TMR compared to bilayer and trilayer cases.

The RMCD of four-layer CrI3 also shows intermediate plateaus at about half the values in the fully aligned states (Fig. 4, B and F, and fig. S10), corresponding to magnetic states with half the net magnetization of the fully aligned states. There are four possible magnetic states for the positive field plateau:  $M_{+}\{\uparrow\downarrow\uparrow\uparrow, \uparrow\uparrow\downarrow\uparrow,$  $\downarrow\uparrow\uparrow\uparrow, \uparrow\uparrow\uparrow\downarrow$ }, the four time-reversal copies ( $M_{-}$ ) being the negative field counterparts (Fig. 4D). The resulting spin-filter configuration should then correspond to one layer polarized opposite to the other three.

Remarkably, in the range of fields where these 1:3 configurations occur, the tunneling current displays multiple plateaus. The green curve in Fig. 4A shows three distinct intermediate  $I_t$  plateaus. Two are in the positive field corresponding to the same intermediate +18% RMCD plateau, and one is in the negative field range. The orange curve, sweeping in the opposite direction, is the time-reversal copy of the green one. The possibility of lateral domains with different net magnetizations being the cause of these extra plateaus is inconsistent with field-dependent RMCD maps of all three measured four-layer CrI<sub>3</sub> sf-MTJs, none of which showed appreciable domains (27). In addition, the tunnel junction

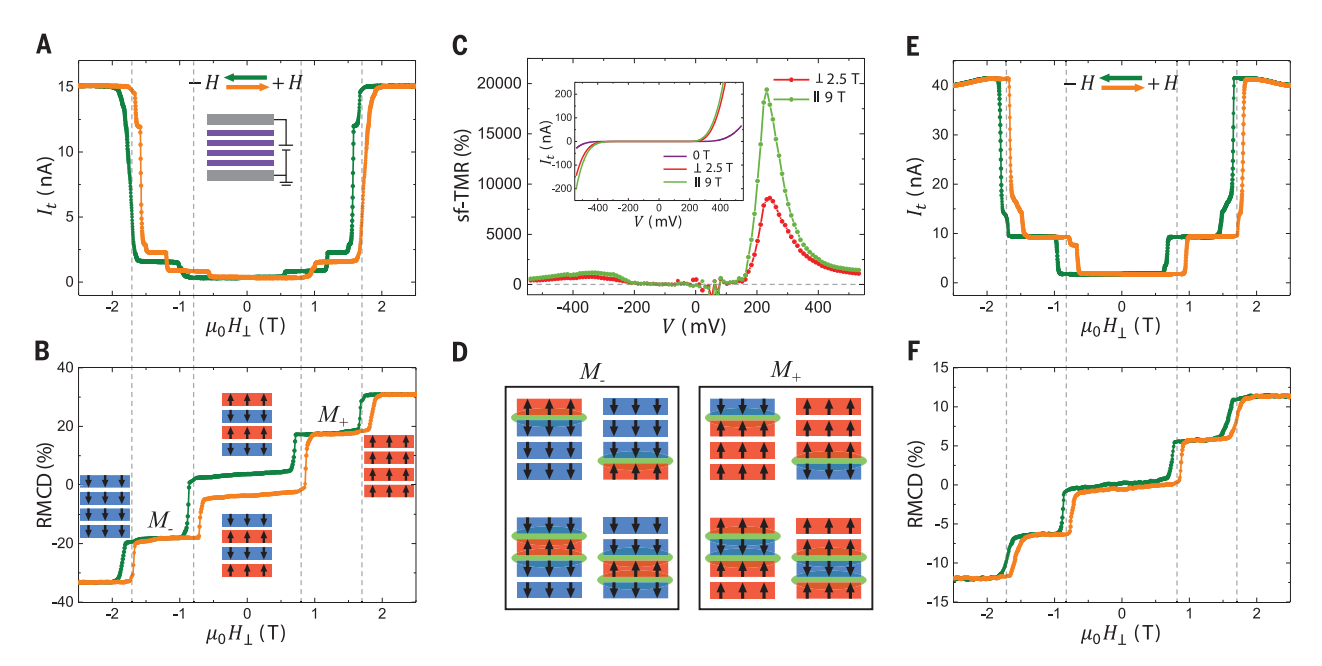


Fig. 4. Four-layer Crl<sub>3</sub> sf-MTJs with extraordinarily large sf-TMR and multiple resistance states. (A) Tunneling current as a function of outof-plane magnetic field ( $\mu_0H_1$ ) at a selected bias voltage (300 mV) and (B) the corresponding RMCD of the same device at zero bias. Insets show the corresponding magnetic states. The junction area is about 2.2 µm<sup>2</sup>.

(C) Calculated sf-TMR ratio as a function of bias based on the  $l_t$ -V curves in the inset. (D) Schematic of possible magnetic states corresponding to the intermediate plateaus in (A) and (B). Green lines show the current-blocking interfaces. (E) and (F) Tunneling current and RMCD from another four-layer Crl<sub>3</sub> sf-MTJ. The junction area is about 1.3 µm<sup>2</sup>.

area is quite small compared with the typical domain size of a few microns in  $CrI_3$  (3, 4).

Instead, these current plateaus probably originate from distinct magnetic states. Whereas the four states in  $M_{+}$  are indistinguishable in RMCD because of the same net magnetization, the tunneling current is likely to be sensitive to the position of the one layer with minority magnetization. First, the  $\downarrow\uparrow\uparrow\uparrow$  and  $\uparrow\uparrow\uparrow\downarrow$  have only one current-blocking interface, whereas ↑↓↑↑ and ↑↑↓↑ have two (green lines between adjacent layers with opposite magnetizations shown in Fig. 4D). Second, the current flow direction as well as the possibly asymmetric few-layer graphene contacts may introduce distinct sf-TMR either between the  $\uparrow\downarrow\uparrow\uparrow$  and  $\uparrow\uparrow\downarrow\uparrow$  states or between the  $\downarrow\uparrow\uparrow\uparrow$  and  $\uparrow\uparrow\uparrow\downarrow$  states (27). This asymmetry may also help to stabilize ↓↑↑↑ and ↑↑↑↓, which in general have higher energy than  $\uparrow\downarrow\uparrow\uparrow$  and  $\uparrow\uparrow\downarrow\uparrow$  in fully symmetric four-layer CrI<sub>3</sub>. However, to identify the specific magnetic states corresponding to the current plateaus will require a means to distinguish the magnetization of individual layers (27).

The four-layer CrI3 sf-MTJ points to the potential for using layered antiferromagnets for engineering multiple magnetoresistance states in an individual sf-MTJ. Figure 4, E and F, and fig. S10 show  $I_t$  and RMCD for two other fourlayer CrI<sub>3</sub> sf-MTJs. They exhibit one or two intermediate plateaus, rather than the three observed in Fig. 4A. The sample dependence suggests that these intermediate states are sensitive to the environment of the CrI<sub>3</sub>, such as the details of the contacts, implying potential tunability-for example, by electro-

statically doping the graphene contacts. One exciting future direction could be to seek electrically controlled switching between several different magnetoresistance states. Already the sf-TMR of up to 19,000% observed in four-layer devices is an order of magnitude larger than that of MgO-based conventional MTJs (19-21) and several orders of magnitude larger than achieved with existing sf-MTJs under similar experimental conditions (12). Although the demonstrated vdW sf-MTJs only work at low temperatures, these results highlight the potential of 2D magnets and their heterostructures for engineering novel spintronic devices with unrivaled performance (33, 34).

## **REFERENCES AND NOTES**

- 1. A. K. Geim, I. V. Grigorieva, Nature 499, 419-425 (2013).
- 2. K. S. Novoselov, A. Mishchenko, A. Carvalho, A. H. Castro Neto, Science 353 aac9439 (2016)
- 3. B. Huang et al., Nature 546, 270-273 (2017).
- 4. D. Zhong et al., Sci. Adv. 3, e1603113 (2017).
- C. Gong et al., Nature 546, 265-269 (2017).
- M. A. McGuire, H. Dixit, V. R. Cooper, B. C. Sales, Chem. Mater. 27, 612-620 (2015)
- M.-W. Lin et al., J. Mater. Chem. C. 4, 315-322 (2016).
- 8. Y. Tian, M. J. Gray, H. Ji, R. J. Cava, K. S. Burch, 2D Mater. 3, 025035 (2016).
- 9. X. Wang et al., 2D Mater. 3, 031009 (2016).
- 10. J.-U. Lee et al., Nano Lett. 16, 7433-7438 (2016).
- 11. D. C. Worledge, T. H. Geballe, J. Appl. Phys. 88, 5277-5279 (2000).
- 12. G.-X. Miao, M. Müller, J. S. Moodera, Phys. Rev. Lett. 102, 076601 (2009). 13. M. N. Baibich et al., Phys. Rev. Lett. 61, 2472-2475 (1988).
- 14. G. Binasch, P. Grünberg, F. Saurenbach, W. Zinn, Phys. Rev. B 39, 4828-4830 (1989).
- 15. B. Dieny et al., Phys. Rev. B 43, 1297-1300 (1991).
- 16. M. Julliere, Phys. Lett. A 54, 225-226 (1975).
- 17. J. S. Moodera, L. R. Kinder, T. M. Wong, R. Meservey, Phys. Rev. Lett. 74, 3273-3276 (1995).

- 18. T. Miyazaki, N. Tezuka, J. Magn. Magn. Mater. 139, L231-L234 (1995).
- S. Yuasa, T. Nagahama, A. Fukushima, Y. Suzuki, K. Ando, Nat. Mater. 3, 868-871 (2004).
- 20. S. S. P. Parkin et al., Nat. Mater. 3, 862-867 (2004).
- 21. S. Ikeda et al., Appl. Phys. Lett. 93, 082508 (2008).
- 22. L. Britnell et al., Science 335, 947-950 (2012).
- 23. G.-H. Lee et al., Appl. Phys. Lett. 99, 243114 (2011). 24. T. Georgiou et al., Nat. Nanotechnol. 8, 100-103 (2013).
- 25. A. Soumyanarayanan, N. Reyren, A. Fert, C. Panagopoulos,
- Nature 539, 509-517 (2016).
- 26. S. A. Wolf et al., Science 294, 1488-1495 (2001).
- 27. See the supplementary materials.
- 28. T. R. McGuire, R. I. Potter, IEEE Trans. Magn. 11, 1018-1038 (1975)
- 29. O. Hellwig, T. L. Kirk, J. B. Kortright, A. Berger, E. E. Fullerton, Nat. Mater. 2, 112-116 (2003).
- 30. O. Hellwig, A. Berger, E. E. Fullerton, Phys. Rev. Lett. 91, 197203 (2003).
- 31. B. Chen et al., Science 357, 191-194 (2017).
- 32. M. Charilaou, C. Bordel, F. Hellman, Appl. Phys. Lett. 104, 212405 (2014)
- 33. D. C. Ralph, M. D. Stiles, J. Magn. Magn. Mater. 320, 1190-1216
- 34. D. MacNeill et al., Nat. Phys. 13, 300-305 (2017).

#### **ACKNOWLEDGMENTS**

We thank Y. Cui, G. Miao, and S. Majetich for insightful discussion. Funding: Work at the University of Washington was mainly supported by the Department of Energy, Basic Energy Sciences, Materials Sciences and Engineering Division (DE-SC0018171). Device fabrication and part of transport measurements are supported by NSF-DMR-1708419, NSF MRSEC 1719797, and UW Innovation Award, D.H.C.'s contribution is supported by DE-SC0002197. Work at CMU is supported by DOE BES DE-SC0012509. Work at HKU is supported by the Croucher Foundation (Croucher Innovation Award), UGC of HKSAR (AoE/P-04/08), and the HKU ORA. Work at ORNL (M.A.M.) was supported by the U.S. Department of Energy, Office of Science, Basic Energy Sciences, Materials Sciences and Engineering Division. K.W. and T.T. acknowledge support from the Elemental Strategy Initiative conducted by the MEXT, Japan, and JSPS KAKENHI grant number JP15K21722. D.X. acknowledges the support of a Cottrell Scholar Award. X.X.

acknowledges the support from the State of Washington-funded Clean Energy Institute and from the Boeing Distinguished Professorship in Physics. Author contributions: W.Y. and X.X. conceived the project. T.S. and X.C. fabricated the devices and performed the experiments, assisted by B.H., N.P.W., K.L.S., and L.Z., supervised by X.X., W.Y., D.X., and D.H.C. T.S. and X.X. analyzed L.Z., supervised by A.A., W.T., D.A., aird D.I.D. 13. aird A.A. alrayzed the data, with theory support from M.W.-Y.T., W.Y., X.Z., and D.X. M.A.M. provided and characterized bulk Crl<sub>3</sub> crystals. T.T. and K.W. provided and characterized bulk hBN crystals. T.S., X.X., W.Y., D.X., and D.H.C.

wrote the manuscript, with input from all authors.  $\mbox{\bf Competing}$  $\mbox{\it interests:}\ \mbox{\sc A}$  provisional patent based on the content of this paper has been filed on behalf of the authors. Data availability: All data files are available from Harvard Dataverse at https://doi.org/10. 7910/DVN/TOTIWA.

### SUPPLEMENTARY MATERIALS

www.sciencemag.org/content/360/6394/1214/suppl/DC1 Materials and Methods

Supplementary Text Figs. S1 to S11 Table S1 References (35-39)

20 November 2017; accepted 24 April 2018 Published online 3 May 2018 10.1126/science.aar4851



# Giant tunneling magnetoresistance in spin-filter van der Waals heterostructures

Tiancheng Song, Xinghan Cai, Matisse Wei-Yuan Tu, Xiaoou Zhang, Bevin Huang, Nathan P. Wilson, Kyle L. Seyler, Lin Zhu, Takashi Taniguchi, Kenji Watanabe, Michael A. McGuire, David H. Cobden, Di Xiao, Wang Yao and Xiaodong Xu

Science 360 (6394), 1214-1218.

DOI: 10.1126/science.aar4851originally published online May 3, 2018

An intrinsic magnetic tunnel junction

An electrical current running through two stacked magnetic layers is larger if their magnetizations point in the same direction than if they point in opposite directions. These so-called magnetic tunnel junctions, used in electronics, must be carefully engineered. Two groups now show that high magnetoresistance intrinsically occurs in samples of the layered material Crl 3 sandwiched between graphite contacts. By varying the number of layers in the samples, Klein *et al.* and Song *et al.* found that the electrical current running perpendicular to the layers was largest in high magnetic fields and smallest near zero field. This observation is consistent with adjacent layers naturally having opposite magnetizations, which align parallel to each other in high magnetic fields.

Science, this issue p. 1218, p. 1214

ARTICLE TOOLS http://science.sciencemag.org/content/360/6394/1214

SUPPLEMENTARY http://science.sciencemag.org/content/suppl/2018/05/02/science.aar4851.DC1

RELATED http://science.sciencemag.org/content/sci/360/6394/1218.full

REFERENCES This article cites 37 articles, 5 of which you can access for free

http://science.sciencemag.org/content/360/6394/1214#BIBL

PERMISSIONS http://www.sciencemag.org/help/reprints-and-permissions

Use of this article is subject to the Terms of Service